Probing the Caveolin-1 P132L Mutant: Critical Insights into Its Oligomeric Behavior and Structure

ARTICLE *in* BIOCHEMISTRY · APRIL 2012

Impact Factor: 3.02 · DOI: 10.1021/bi3001853 · Source: PubMed

3 AUTHORS, INCLUDING:

Monica D. Rieth
Lehigh University
2 PUBLICATIONS **10** CITATIONS
SEE PROFILE

Kerney Jebrell Glover
Lehigh University
22 PUBLICATIONS **782** CITATIONS
SEE PROFILE

Published in final edited form as:
Biochemistry. 2012 May 8; 51(18): 3911–3918. doi:10.1021/bi3001853.

Probing the caveolin-1 P132L mutant: Critical insights into its oligomeric behavior and structure

Monica D. Rieth[†], **Jinwoo Lee**[†], and **Kerney Jebrell Glover**[*]
Department of Chemistry, Lehigh University, 6 E. Packer Ave, Bethlehem, Pennsylvania 18015, USA

Abstract

Caveolin-1 is the most important protein found in caveolae, which are cell surface invaginations of the plasma membrane that act as signaling platforms. A single point mutation in the transmembrane domain of caveolin-1 (proline 132 to leucine) has deleterious effects on caveolae formation in vivo, and has been implicated in various disease states, particularly aggressive breast cancers. Using a combination of gel filtration chromatography and analytical ultracentrifugation we found that a fully-functional construct of caveolin-1 ($Cav1_{62–178}$) was a monomer in dodecylphosphocholine micelles. In contrast, the P132L mutant of $Cav1_{62–178}$ was dimeric. To explore the dimerization of the P132L mutant further, various truncated constructs ($Cav1_{82–178}$, $Cav1_{96–178}$, $Cav1_{62–136}$, $Cav1_{82–136}$, $Cav1_{96–136}$) were prepared which revealed that oligomerization occurs in the transmembrane domain (residues 96–136) of caveolin-1. To characterize the mutant structurally, solution-state NMR experiments in *lyso*-myristoylphosphatidylglycerol were undertaken of the $Cav1_{96–136}$ P132L mutant. Chemical shift analysis revealed that compared to the wild type, helix 2 in the transmembrane domain was lengthened by four residues (wild type, residues 111 to 129; mutant, residues 111–133), which corresponds to an extra turn in helix 2 of the mutant. Lastly, point mutations at position 132 of $Cav1_{62–178}$ (P132A, P132I, P132V, P132G, P132W, P132F) revealed that no other hydrophobic amino acid can preserve the monomeric state of $Cav1_{62–178}$ which indicates that proline 132 is critical in supporting proper caveolin-1 behavior.

Keywords

caveolin; caveolae; analytical ultracentrifugation; gel filtration; NMR; oligomerization; secondary structure

Caveolae are indentations of the plasma membrane of mammalian cells that are approximately 50–100 nm in diameter (1). These microdomains are intimately involved in numerous cellular functions ranging from signal transduction to lipid recycling (2). Caveolae are ubiquitous, and can be found in most terminally differentiated cell types, notably smooth muscle cells and adipocytes (1). Caveolae are primarily comprised of a protein called caveolin, which is critical for the formation of caveolae. It is estimated that approximately 100–200 caveolin proteins are present in a single caveola, and studies have shown that when the caveolin gene is silenced, caveolae disappear from the surface of cells (3, 4). Caveolin is an integral membrane protein, and approximately 50% of the polypeptide

[*]Correspondence should be addressed to Kerney Jebrell Glover, phone: 1-610-758-5081; Fax: 1-610-758-6536; kjg206@lehigh.edu.
[†]The authors contributed equally to the work presented in this paper.

Supporting Information
TALOS+ data (Table 1) is available for wild-type $Cav1_{96–136}$. This material is available free of charge via the Internet at http://pubs.acs.org.

chain is predicted to interact with the plasma membrane. Glycosylation mapping, limited proteolysis, and cell surface biotinylation studies have demonstrated that the N- and C-termini of caveolin reside on the cytosolic side of the membrane (5, 6, 7). The transmembrane region of caveolin is approximately 33 amino acids in length, which is significantly longer than the 20–25 amino acids required to span the plasma membrane. In addition, there are no soluble amino acids present in the transmembrane region of caveolin that would facilitate a polytopic orientation. Taken together, these findings have led to the postulation that caveolin forms a horseshoe-like loop in the membrane (Figure 1). The horseshoe-like loop conformation is believed to facilitate the high degree of membrane curvature observed in caveolae (4). Furthermore, the membrane curvature is believed to be stabilized by the formation of high molecular weight caveolin oligomers.

Caveolin has been closely linked to a number of disease states including heart disease, Alzheimer's, and cancer. Specifically, a naturally occurring point mutation (P132L) in the caveolin-1 gene is present in approximately 16% of breast cancers, and has been closely linked to increased recurrence and metastasis (8, 9). In addition, this mutant appears to be functionally different from the wild-type as it is retained in the Golgi apparatus of cells and does not get transported to its final destination in the plasma membrane. The expression of the P132L mutant results in the elimination of caveolae from the surface of cells (10). Interestingly, the P132L mutant appears to behave in a dominant negative manner: When both the P132L mutant and wild-type caveolin are co-expressed, both become localized to the Golgi, which is a fate common to misfolded proteins (10). Furthermore, a study by Bonuccelli et al demonstrates that when caveolin-1 P132L is expressed in Met-1 cells, it acts as a loss-of-function mutation and promotes recurrence of breast cancer (8).

In this report, we examine both the oligomeric and secondary structural changes that occur in the caveolin-1 P132L mutant versus wild-type caveolin-1. Using gel filtration chromatography and sedimentation equilibrium analytical ultracentrifugation we show that the P132L mutant is dimeric compared to the wild-type which is monomeric. Using various truncated constructs, we have isolated the dimerization region to the transmembrane domain which is where the P132L mutation resides. In addition, we show that substitution of proline 132 with 6 other nonpolar amino acids does not disrupt dimerization, which reveals the importance of proline at position 132. Using chemical shift indexing NMR analysis we found that the putative re-entrant helix of the P132L mutant is extended by 4 additional amino acids which results in a longer α-helix when compared to the wild-type. Furthermore, the NMR studies reveal that the P132L point mutation results in only a localized change to the transmembrane region of caveolin rather than a global conformation change.

Materials and Methods

Protein Expression and Purification

The DNA for $Cav1_{62–178}$ was synthesized by Genscript Corporation (Piscataway, NJ). Caveolin-1 has three sites of cysteine palmitoylation (C133, C143, C156) that have been shown to be nonessential for proper caveolin-1 folding and trafficking (11, 12, 13). Therefore, each cysteine was mutated to serine to avoid unwanted and biologically irrelevant disulfide bonding. The $Cav1_{62–178}$ gene was cloned, over-expressed, and purified as described in Diefenderfer et al (14). After HPLC purification, 30 mg of dried $Cav1_{62–178}$ was dissolved in 3 mL of hexafluoroisopropanol followed by the addition of 7 mL of deionized water. The solution was flash frozen and lyophilized. MALDI-TOF analysis confirmed the identity of the final protein product. The truncated wild-type and P132L mutant constructs prepared were: $Cav1_{82–178}$, $Cav1_{82–136}$, $Cav1_{96–178}$, $Cav1_{96–136}$, $Cav1_{62–136}$. The point mutation constructs prepared were $Cav1_{62–178}$: P132A, P132G,

P132W, P132F, P132V, P132I. The truncated and point mutation constructs were expressed and purified using the same procedure described above.

Expression of Isotopically Labeled Protein

The expression of uniformly labeled ^{15}N and ^{13}C $Cav1_{96–136}$ P132L was prepared as described in Marley et al (15). Labeled amino acids were incorporated by expressing $Cav1_{96–136}$ P132L according to the procedure outlined in Truhlar et al (16).

Gel Filtration Chromatography

To 0.8 mg of lyophilized $Cav1_{62–178}$, 1.0 mL of buffer (20 mM HEPES pH 7.4, 150 mM NaCl, and 50 mM DPC (Anatrace, Maumee, OH)) was added followed by three minutes of vigorous vortexing. Next, the resultant clear solution was filtered through a 0.2 μm spin filter and injected onto a Sephacryl-300HR 16/60 column (GE Healthcare, Piscataway, NJ) equilibrated with buffer (20 mM HEPES pH = 7.4, 150 mM NaCl and 5 mM DPC). The column was calibrated using alcohol dehydrogenase, carbonic anhydrase, α-amylase, bovine serum albumin, and cytochrome c oxidase, and the elution profile was monitored at 280 nm. All truncated and point mutation constructs were run in an identical fashion to the wild-type and mutant $Cav1_{62–178}$.

Analytical Ultracentrifugation

0.8 mg of lyophilized $Cav1_{62–178}$ was reconstituted into a density-matched buffer comprised of 20 mM HEPES pH 7.4, 100 mM NaCl, 50 mM DPC and 52.5 % (v/v) D_2O. DPC micelles were matched using a D_2O concentration of 52.5% (v/v) in a solution of 20 mM HEPES 100 mM NaCl pH = 7.4 (17). Each protein sample was prepared at three concentrations (30 μM, 15 μM, and 7.5 μM), and verified using the BCA Assay (Pierce Protein Research Products, Rockford IL). The samples were loaded into a sixsector charcoal-filled epon centerpiece (path length 1.2 cm) using the DPC buffer solution above without protein as the reference solution. The volume of sample per sector was 120 μL. The cells were loaded in a Beckman Ti-60 4-hole rotor. Equilibrium absorbance measurements were taken at three speeds, and the data were analyzed by global nonlinear least squares fitting using the computer program “HeteroAnalysis Version 1.1.0.44 - beta” (University of Connecticut) (18). $Cav1_{62–178}$ was fit to the ideal model to obtain the weight-averaged molecular weight of the protein. During fitting, all parameters (molecular weight, baseline, and reference concentration) were allowed to float. Mutant $Cav1_{62–178}$ P132L was fit to a “Monomer-Nmer” model (where N was fixed to a value of 2). Again, all parameters (molecular weight, baseline, and reference concentration) were allowed to float. The partial specific volumes of the wild-type and mutant $Cav1_{62–178}$ were calculated using established methodology (0.7603 mL/g and 0.7615 mL/g, respectively) (19). The density of the DPC buffer (1.0592 g/mL) was determined using a Kyoto Electronics Density/Specific Gravity Meter (model #DA-210).

NMR Sample Preparation

To 2.5 mg of lyophilized $Cav1_{96–136}$ P132L, 500 μL of LMPG buffer was added (100 mM LMPG, 100 mM NaCl 20 mM phosphate pH 7, 10% D_2O) for a final protein concentration of 1 mM. The sample was vortexed vigorously and briefly heated (approximately 1 minute) in a water bath until clear. The clear solution was spin filtered in a 0.2 μm filter to remove any particulates. The NMR spectrum was acquired at 37°C using a 600 MHz Bruker Advance II NMR spectrometer (Billerica, MA) equipped with a cryoprobe. For backbone assignments TROSY-based HSQC, HNCA, HN(CO)CA experiments were performed. Specific amino acid labeling (valine, serine, leucine) was used to clarify ambiguous peaks. The spectra were processed using NMRPipe and Sparky (20, 21). Secondary structure

information was obtained using Cα chemical shifts as described in Wishart et al (22). Dihedral angles for wild-type $Cav1_{96–136}$ were obtained using the computer program TALOS+ (23). For TALOS+ H, N, CO, Cα, Cβ chemical shift data were used.

Results and Discussion

For studies of caveolin-1 oligomerization we chose a construct that encompasses residues 62–178 ($Cav1_{62–178}$). *In vivo* studies have shown that when the first 65 amino acids were deleted from caveolin-1, it had a behavior that was indistinguishable from that of the full-length protein (24). This strongly indicates that $Cav1_{62–178}$ retains the crucial structural elements necessary for full caveolin-1 function.

Wild-type $Cav1_{62–178}$ was reconstituted into a buffer containing dodecylphosphocholine (DPC) micelles. DPC micelles are a very native-like membrane mimic that is used widely in a variety of biophysical membrane protein experiments (25, 26, 27). When reconstituted $Cav1_{62–178}$ was subjected to gel filtration analysis, a single symmetrical peak was observed (Figure 2A-solid line). The presence of a single symmetrical peak indicates that a homogenous oligomeric population of the protein is present, and that $Cav1_{62–178}$ is *not* forming multiple oligomeric states. In addition, $Cav1_{62–178}$ did not elute in the void volume, revealing that the column retained separation ability. Therefore, if multiple $Cav1_{62–178}$ oligomeric states were present, gel filtration would have resolved them. When the gel filtration column was calibrated with known globular protein standards, the $Cav1_{62–178}$ fraction had an apparent molecular weight of 115 kDa. Based on these results, caveolin-1 forms only one predominant oligomeric state.

Next, mutant $Cav1_{62–178}$ P132L was subjected to gel filtration analysis. The mutant also eluted as a single, symmetrical, non-voided peak indicating that a homogenous oligomeric population was present (Figure 2A- dashed line). However, the mutant eluted before the wild-type indicating that it was present in a larger oligomeric state. In contrast to the wild-type, the mutant had an apparent molecular weight of 190 kDa. However, gel filtration analysis does not give us definitive information about the precise oligomeric state of the wild-type and mutant $Cav1_{62–178}$: This is due to the fact that DPC molecules are bound to $Cav1_{62–178}$, which can dramatically inflate the apparent molecular weight. Also, membrane protein-detergent complexes may not be globular, which can inflate the molecular weight as well.

To overcome the limitations of gel filtration analysis, wild-type and mutant $Cav1_{62–178}$ were subjected to analysis by analytical ultracentrifugation. The method of sedimentation equilibrium was employed because it is a very powerful approach for determining the molecular weight of membrane proteins in detergent solutions. Importantly, sedimentation equilibrium experiments give molecular weight information that is independent of molecular shape. In addition, sedimentation equilibrium experiments can be run under density-matched conditions, which allows for the detergent contribution to the observed molecular weight to be eliminated (28, 29, 30). Therefore, using this method, the exact oligomeric state of wild-type and mutant $Cav1_{62–178}$ can be characterized.

Figure 3 summarizes the data from the analytical ultracentrifugation experiments of both the wild-type and the P132L mutant. For wild-type $Cav1_{62–178}$ (Figure 3 A–C), the data were fit to the ideal, single species model. It was clear from the gel filtration experiments that only one oligomeric population was present for both the wild-type and mutant $Cav1_{62–178}$. After fitting the sedimentation profile of $Cav1_{62–178}$ to the ideal model, the reported molecular weight was 14,606 ± 19 Da. This value is reported with 617 degrees of freedom and a root mean square deviation of 0.01135. This agrees very well with the calculated molecular

weight of the wild-type monomer which is 13,450 Da (The ~1 kDa discrepancy can be attributed to the inherent inaccuracy of predicting partial specific volumes of proteins in detergent solutions). Based on these results it is clear that caveolin-1 is a monomer, and does not homo-oligomerize at all. Therefore, it is unlikely that the observed SDS-resistant high molecular weight complexes previously reported for caveolin-1 are simply a result of caveolin-1 homo-oligomerizing (6). Clearly, the mechanism of caveolae formation is more complex and likely involves other biomolecules such as cholesterol. In fact, caveolin-1 has been shown to closely associate with cholesterol *in vivo*; therefore, the appearance of these high molecular weight complexes may be due to the presence of SDS resistant caveolin-cholesterol aggregates (6). It is important to note that SDS is a much more powerful detergent towards protein deaggregation than DPC, which is much milder. Considering this, it is highly unlikely that DPC would interfere with caveolin-1 oligomerization. Additionally, studies suggesting caveolin-1 oligomerizes are based heavily on the behavior of fragments of caveolin from the N-terminal and scaffolding domains (6, 24, 31). It is not clear from these studies whether the fragments were representative of the native caveolin-1 protein. In one report the studies were performed in the absence of a membrane mimic which is not representative of caveolin-1's membrane environment. Our studies reveal that when a *fully-functional* construct of caveolin-1 ($Cav1_{62–178}$) is analyzed in a membrane environment it does not form high-order oligomers and is in fact monomeric. This result helps to clarify the role of caveolin-1 in caveolae.

Next, mutant $Cav1_{62–178}$ P132L was subjected to analysis by analytical ultracentrifugation (Figure 3D–F). Initially, the data were fitted to the ideal species model the same way that the wild type data were fitted. The observed molecular weight was 28,282 Da. This value is approximately twice the molecular weight of the P132L monomer, 13,465 Da, showing that a dimeric species was present. Next, we explored the possibility of a monomer-dimer equilibrium by fitting the data to a monomer-dimer model. Upon fitting, the observed molecular weight of the monomer was 14,079 ± 55 Da. This value is reported with 1420 degrees of freedom and a root mean square deviation of 0.01515. This number corresponds very well to the calculated molecular weight of the P132L monomer (13,465 Da). In addition, the model produced a dissociation constant of 15 nM, which shows that the dimer is quite stable. We take this dissociation constant to be the upper limit. We believe the dissociation constant is actually much less than 15 nM because at the concentrations used in these studies no monomeric caveolin-1 was observed. From these results, we conclude that the P132L mutant forms stable dimers in a membrane-like environment unlike the wild-type which is monomeric.

After determining that the oligomeric state of the P132L mutant was dimeric, the region of $Cav1_{62–178}$ P132L that was responsible for the observed dimerization was investigated. Caveolin-1 is typically described as having four distinct domains: an N-terminal domain (residues 62–81), a scaffolding domain (residues 82–95), a transmembrane domain (residues 96–136), and a C-terminal domain (residues 137–178). Therefore, the following truncated constructs of both the wild-type and mutant caveolin-1 were generated: $Cav1_{62–136}$, $Cav1_{82–136}$, $Cav1_{82–178}$, $Cav1_{96–136}$, and $Cav1_{96–178}$. Importantly, all constructs contained the intact transmembrane domain (residues 96–136). Each of the five constructs was analyzed by gel filtration chromatography, and the elution profiles of both wild-type and P132L were compared (Figure 2B–F). In all five cases, the P132L mutant elutes before the wild-type indicating that a larger oligomeric species was present. Since all of the truncated constructs contained the intact transmembrane domain, and all truncated constructs elute before the wild-type, these results indicate that the dimerization region lies in the transmembrane domain of caveolin-1 where the P132L mutation is found.

Next, NMR structural studies were undertaken to observe the changes that occur in the transmembrane domain of the wild-type versus the P132L mutant. Figure 4 shows the HSQC spectrum of mutant $Cav1_{96–136}$ P132L. Linewidths are broader when compared to the wild-type spectrum reported in Lee et al (32). This observed line broadening is consistent with oligomerization. When the N, H, CO, Cα, and Cβ chemical shifts for the wild-type $Cav1_{96–136}$ were inputted into the computer program TALOS+, residues Y95-V131 were confidently predicted to have a dihedral angle, and residues P132-K135 were predicted to be dynamic (23). Table 1 in the Supplementary Information provides a complete list of the TALOS+ data. Importantly, the prediction of the wild-type secondary structure in TALOS+ matched the secondary structure prediction using only Cα chemical shift data. Therefore, we used the Cα chemical shift indexing to reveal the secondary structure of $Cav1_{96–136}$ P132L. Chemical shift indexing (Figure 5) of Cα reveals that the transmembrane domain still retains the four distinct regions previously observed for the wild-type caveolin transmembrane domain: There is an α-helix from residues 97–107 (helix 1), a break from residues 108–110, another α-helix from residues 111–129 (helix 2), and an unstructured region from residues 130–136 (32). Consistent with the horseshoe topology model of caveolin, the break at residues 108–110 is likely where the turn occurs so that the polypeptide chain can return to the membrane surface. Clearly in the case of the mutant, the break is not lost so it is unlikely that this mutant disrupts the proposed horseshoe topology. In addition, helix 1 is unaffected as well. However, helix 2 is extended by 4 residues to encompass residues 111–133. Therefore, there is approximately one extra helical turn in the mutant. The unstructured region now begins at residue 134 for the mutant rather than residue 130 for the wild-type. This increased helicity is likely forming a dimerization domain in the transmembrane domain in close proximity to position 132 (Figure 6). In the native protein, residue P132 causes helix 2 to terminate at residue 129 which prevents the dimerization from occurring. Therefore, the helix-breaking tendency of proline is employed to prevent the dimerization of caveolin-1. Figure 6 shows a model of how caveolin-1 dimerization may occur. This model is an extension of the original model of caveolin-1 presented by Hancock and Parton, which was based entirely on primary sequence analysis and not on biophysical data (4). Our model shows that when the proline is removed from position 132 the unstructured region begins at residue 134 instead of residue 130. We believe this lengthening of helix 2 opens up an interface that leads to the dimerization of caveolin-1, which was observed in the analytical ultracentrifugation study. The purpose of our model is to highlight this dimerization interface. Although other dimerization models consistent with the association around position 132 can be built, we present only one model for brevity. Clearly, more studies to definitively characterize the structure of the dimer will be needed.

Next, specific hydrophobic amino acid substitutions were made at position 132 to determine whether other hydrophobic amino acids could substitute for proline at the 132 position. We chose to substitute the following residues: isoleucine (P132I), valine (P132V), alanine (P132A), glycine (P132G), tryptophan (P132W), phenylalanine (P132F). Each residue is non-polar so it does not affect the properties of $Cav1_{62–178}$ by significantly changing the hydrophobicity. Each of these mutants was examined by gel filtration chromatography and compared to the wild-type and mutant $Cav1_{62–178}$. Based on the elution profiles of the mutants, we can see that all of them elute before the wildtype (Figure 7) showing that all of the mutants retain dimerization capabilities. The P132A, P132G, P132I, and P132V mutants had slightly longer retention times compared to the P132L mutant when run at a constant flow rate indicating that the dimerization may be somewhat weaker for some of the point mutants. Clearly, it appears that proline is the only amino acid that is tolerated at position 132, and it further explains why proline is conserved in all three caveolin isoforms.

As stated in the Introduction, the mutation of P132L in caveolin-1 results in a variety of disease states. However, there has been little characterization of the differences between the

wild-type and the mutant at the atomic level. Importantly, our data show that wild-type caveolin-1 is monomeric and does not form high-order oligomers. Therefore, the high-order oligomers that have been reported for caveolin-1 are likely due to other proteins/factors that are present *in vivo*. In contrast, the P132L mutant spontaneously dimerizes. This dimerization could explain why the mutant is retained in the Golgi apparatus *in vivo* and does not reach its final destination in the plasma membrane. Furthermore, it is likely that other factors are at play and are contributing to the creation of the caveolin oligomers observed *in vivo*. Also, given that processes in the cell are tightly regulated, it is reasonable to think that for proper cellular transport caveolin-1 must be in a monomeric state and then once it reaches the plasma membrane other factors such as cholesterol, or the protein PTRF/cavin could trigger the oligomerization. Recent studies have shown that caveolin closely associates with the protein, PTRF/cavin. In fact, when the PTRF/cavin gene is silenced, the number of caveolae in the plasma membrane diminishes (33). The P132L mutant, on the other hand, dimerizes which may not be the proper oligomeric state for trafficking to the plasma membrane, which could explain why it is retained in the Golgi apparatus. Proline is a very unique amino acid because it is conformationally rigid. Because of this rigidity, proline is known to be helix breaking. This could be critical for caveolin-1 as P132 is located towards the end of the transmembrane domain where the protein is transitioning from a near-vertical helix in the membrane to the C-terminal domain, which is an amphipathic helix that is predicted to reside horizontally on the membrane surface. When the proline is removed, the second helix of the transmembrane domain is extended by one turn. This small change is significant enough to open up a dimerization domain helix 2 (Figure 6). No other non-polar amino acids can be substituted for proline, indicating how critical this residue is in supporting proper caveolin-1 behavior.

Supplementary Material

Refer to Web version on PubMed Central for supplementary material.

Acknowledgments

We would like to thank Penn State Hershey College of Medicine for use of their NMR facility. We would also like to thank Dr. Fang Tian for useful NMR discussions.

This work is supported by NIH RO1 GM093258-01A1 grant to K.J.G.

Abbreviations

NMR	nuclear magnetic resonance spectroscopy
DPC	dodecylphosphocholine
LMPG	lysomyristoylphosphatidylglycerol
SDS	sodium dodecylsulfate

References

1. Lisanti MP, Williams TM. The Caveolin Genes: From Biology to Medicine. Annual Medicine. 2004; 36:584–595.
2. Spisni E, Tomasi V, Cestaro A, Tosatto SC. Structural Insights into the Function of Human Caveolin 1. Biochem. Biophys. Res. Commun. 2005; 338:1383–1390. [PubMed: 16263077]
3. Drab M, Verkade P, Elger M, Kasper M, Lohn M, Lauterbach B, Menne J, Lindschau C, Mende F, Luft FC, Schedl A, Haller H, Kurzchalia TV. Loss of Caveolae, Vascular Dysfunction, and

Pulmonary Defects in Caveolin-1 Gene-Disrupted Mice. Science. 2001; 293:2449–2452. [PubMed: 11498544]

4. Parton RG, Hanzal-Bayer M, Hancock JF. Biogenesis of Caveolae: A Structural Model for Caveolin-Induced Domain Formation. J. Cell. Sci. 2006; 119:787–796. [PubMed: 16495479]
5. Monier S, Dietzen DJ, Hastings WR, Lublin DM, Kurzchalia TV. Oligomerization of VIP21-Caveolin in Vitro is Stabilized by Long Chain Fatty Acylation Or Cholesterol. FEBS Lett. 1996; 388:143–149. [PubMed: 8690074]
6. Sargiacomo M, Scherer PE, Tang Z, Kubler E, Song KS, Sanders MC, Lisanti MP. Oligomeric Structure of Caveolin: Implications for Caveolae Membrane Organization. Proc. Natl. Acad. Sci. U. S. A. 1995; 92:9407–9411. [PubMed: 7568142]
7. Dupree P, Parton RG, Raposo G, Kurzchalia TV, Simons K. Caveolae and Sorting in the Trans-Golgi Network of Epithelial Cells. EMBO J. 1993; 12:1597–1605. [PubMed: 8385608]
8. Bonuccelli G, Casimiro MC, Sotgia F, Wang C, Liu M, Katiyar S, Zhou J, Dew E, Capozza F, Daumer KM, Minetti C, Milliman JN, Alpy F, Rio MC, Tomasetto C, Mercier I, Flomenberg N, Frank PG, Pestell RG, Lisanti MP. Caveolin-1 (P132L), a Common Breast Cancer Mutation, Confers Mammary Cell Invasiveness and Defines a Novel Stem cell/metastasis-Associated Gene Signature. Am. J. Pathol. 2009; 174:1650–1662. [PubMed: 19395651]
9. Williams TM, Lisanti MP. Caveolin-1 in Oncogenic Transformation, Cancer, and Metastasis. American Journal of Physiology-Cell Physiology. 2005; 288:C494–C506. [PubMed: 15692148]
10. Lee H, Park DS, Razani B, Russell RG, Pestell RG, Lisanti MP. Caveolin-1 Mutations (P132L and Null) and the Pathogenesis of Breast Cancer - Caveolin-1 (P132L) Behaves in a Dominant-Negative Manner and Caveolin-1 (−/−) Null Mice show Mammary Epithelial Cell Hyperplasia. American Journal of Pathology. 2002; 161:1357–1369. [PubMed: 12368209]
11. Uittenbogaard A, Smart EJ. Palmitoylation of Caveolin-1 is Required for Cholesterol Binding, Chaperone Complex Formation, and Rapid Transport of Cholesterol to Caveolae. J. Biol. Chem. 2000; 275:25595–25599. [PubMed: 10833523]
12. Dietzen DJ, Hastings WR, Lublin DM. Caveolin is Palmitoylated on Multiple Cysteine Residues. Palmitoylation is Not Necessary for Localization of Caveolin to Caveolae. J. Biol. Chem. 1995; 270:6838–6842. [PubMed: 7896831]
13. Sotgia F, Razani B, Bonuccelli G, Schubert W, Battista M, Lee H, Capozza F, Schubert AL, Minetti C, Buckley JT, Lisanti MP. Intracellular Retention of Glycosylphosphatidyl Inositol-Linked Proteins in Caveolin-Deficient Cells. Molecular and Cellular Biology. 2002; 22:3905–3926. [PubMed: 11997523]
14. Diefenderfer C, Lee J, Mlyanarski S, Guo Y, Glover KJ. Reliable Expression and Purification of Highly Insoluble Transmembrane Domains. Anal. Biochem. 2009; 384:274–278. [PubMed: 18929529]
15. Marley J, Lu M, Bracken C. A Method for Efficient Isotopic Labeling of Recombinant Proteins RID A-7811-2009. J. Biomol. NMR. 2001; 20:71–75. [PubMed: 11430757]
16. Truhlar SM, Cervantes CF, Torpey JW, Kjaergaard M, Komives EA. Rapid Mass Spectrometric Analysis of 15N-Leu Incorporation Fidelity during Preparation of Specifically Labeled NMR Samples. Protein Sci. 2008; 17:1636–1639. [PubMed: 18567787]
17. Losonczi JA, Olejniczak ET, Betz SF, Harlan JE, Mack J, Fesik SW. NMR Studies of the Anti-Apoptotic Protein Bcl-xL in Micelles. Biochemistry. 2000; 39:11024–11033. [PubMed: 10998239]
18. Cole JL. Analysis of Heterogeneous Interactions. Methods Enzymol. 2004; 384:212–232. [PubMed: 15081689]
19. Cohn EJ, Edsall JJ. Proteins, Amino Acids, and Peptides as Ions and Dipolar Ions. 1943:375.
20. Goddard, TD.; Kneller, DG. SPARKY 3. San Francisco: University of California;
21. Delaglio F, Grzesiek S, Vuister GW, Zhu G, Pfeifer J, Bax A. NMRPipe: A Multidimensional Spectral Processing System Based on UNIX Pipes. J. Biomol. NMR. 1995; 6:277–293. [PubMed: 8520220]
22. Wishart D, Sykes B. The C-13 Chemical-Shift Index - a Simple Method for the Identification of Protein Secondary Structure using C-13 Chemical-Shift Data. J. Biomol. NMR. 1994; 4:171–180. [PubMed: 8019132]

23. Shen Y, Delaglio F, Cornilescu G, Bax A. TALOS+: A Hybrid Method for Predicting Protein Backbone Torsion Angles from NMR Chemical Shifts. J. Biomol. NMR. 2009; 44:213–223. [PubMed: 19548092]
24. Machleidt T, Li WP, Liu P, Anderson RG. Multiple Domains in Caveolin-1 Control its Intracellular Traffic. J. Cell Biol. 2000; 148:17–28. [PubMed: 10629215]
25. Neumoin A, Arshava B, Becker J, Zerbe O, Naider F. NMR Studies in Dodecylphosphocholine of a Fragment Containing the Seventh Transmembrane Helix of a G-Protein-Coupled Receptor from Saccharomyces Cerevisiae. Biophysical journal. 2007; 93:467–482. [PubMed: 17449670]
26. Zamoon J, Mascioni A, Thomas DD, Veglia G. NMR Solution Structure and Topological Orientation of Monomeric Phospholamban in Dodecylphosphocholine Micelles. Biophys. J. 2003; 85:2589–2598. [PubMed: 14507721]
27. Beswick V, Guerois R, Cordier-Ochsenbein F, Coic YM, Tam HD, Tostain J, Noel JP, Sanson A, Neumann JM. Dodecylphosphocholine Micelles as a Membrane-Like Environment: New Results from NMR Relaxation and Paramagnetic Relaxation Enhancement Analysis. Eur. Biophys. J. 1999; 28:48–58. [PubMed: 9933923]
28. Fleming KG. Determination of Membrane Protein Molecular Weight using Sedimentation Equilibrium Analytical Ultracentrifugation. Chapter 7. Curr. Protoc. Protein Sci. 2008; 7:Unit 7.12.1–Unit 7.12.13.
29. Reynolds J, Tanford C. Determination of Molecular Weight of the Protein Moiety in Protein-Detergent Complexes without Direct Knowledge of Detergent Binding. Proc. Natl. Acad. Sci. 1976; 73:4467–4470. [PubMed: 188041]
30. Mayer G, Ludwig B, Muller H, van den Brook JA, Friesen RHE, Schubert D. Studying Membrane Proteins in Detergent Solution by Analytical Ultracentrifugation: Different Methods for Density Matching. Progr Colloid Polym Sci. 1999; 113:176–181.
31. Fernandez MA, Albor C, Ingelmo-Torres M, Nixon SJ, Ferguson C, Kurzchalia T, Tebar F, Enrich C, Parton RG, Pol A. Caveolin-1 is Essential for Liver Regeneration. Science. 2006; 313:1628–1632. [PubMed: 16973879]
32. Lee J, Glover KJ. The Transmembrane Domain of Caveolin-1 Exhibits a Helix-Break-Helix Structure. Biochim. Biophys. Acta. 2012; 1818:1158–1164. [PubMed: 22240009]
33. Liu L, Brown D, McKee M, Lebrasseur NK, Yang D, Albrecht KH, Ravid K, Pilch PF. Deletion of Cavin/PTRF Causes Global Loss of Caveolae, Dyslipidemia, and Glucose Intolerance. Cell. Metab. 2008; 8:310–317. [PubMed: 18840361]

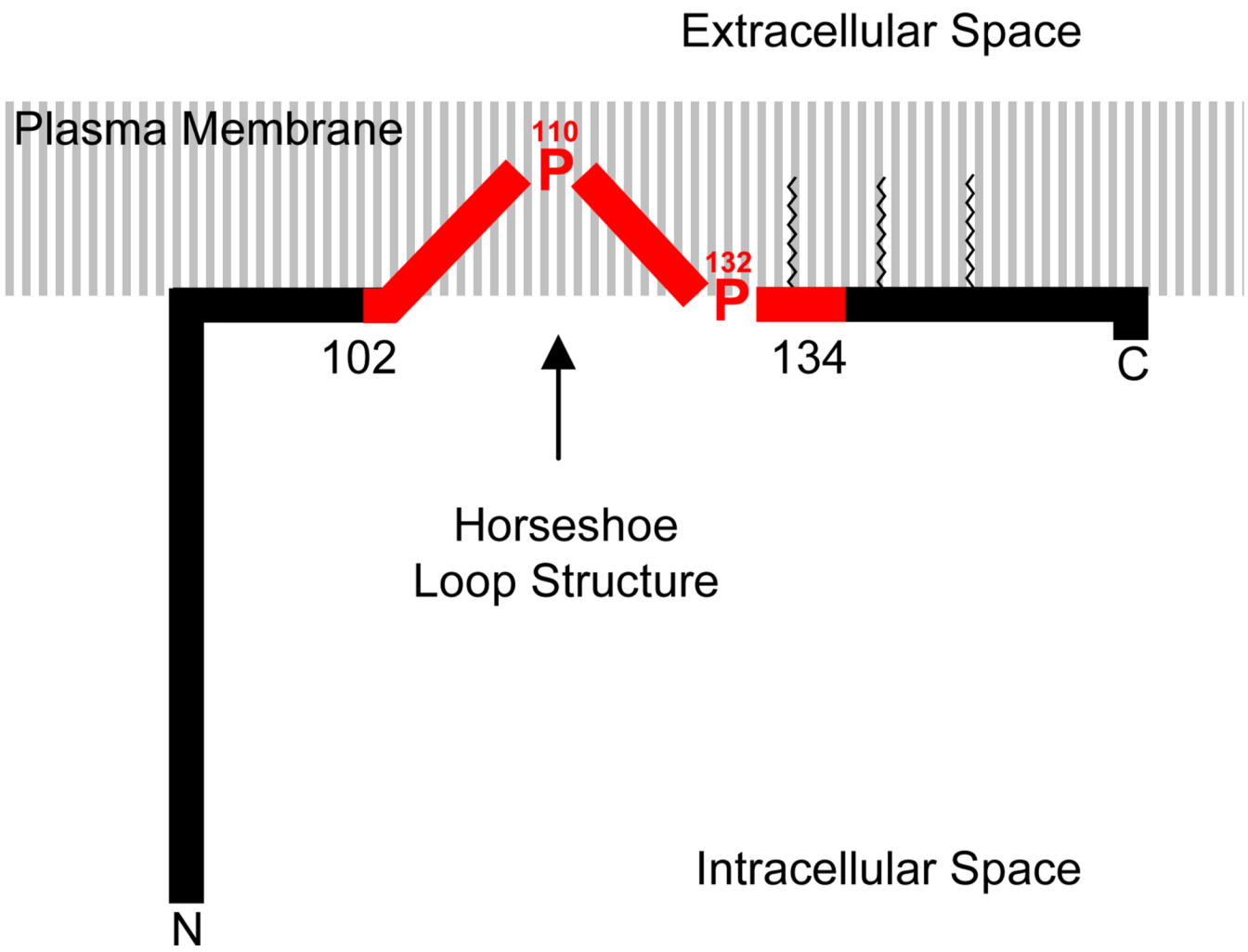

Figure 1.

A) Cartoon of caveolin-1 topology. The transmembrane domain is highlighted in red. The zigzag lines represent sites of cysteine palmitoylation.

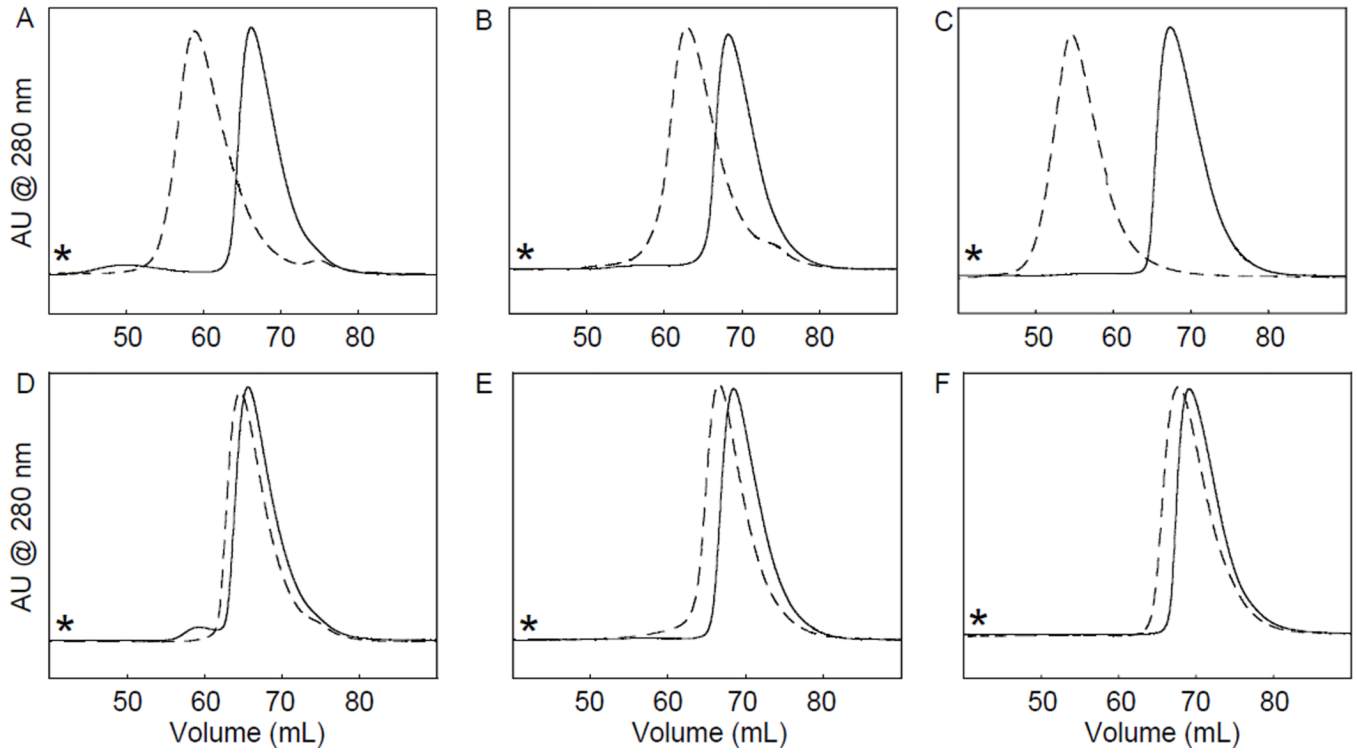

Figure 2.

Gel filtration chromatograms of various caveolin-1 constructs. A) $Cav1_{62–178}$ B) $Cav1_{82–178}$ C) $Cav1_{96–178}$ D) $Cav1_{62–136}$ E) $Cav1_{82–136}$ F) $Cav1_{96–136}$. Solid line represents wild-type. Dashed line represents the P132L mutant.

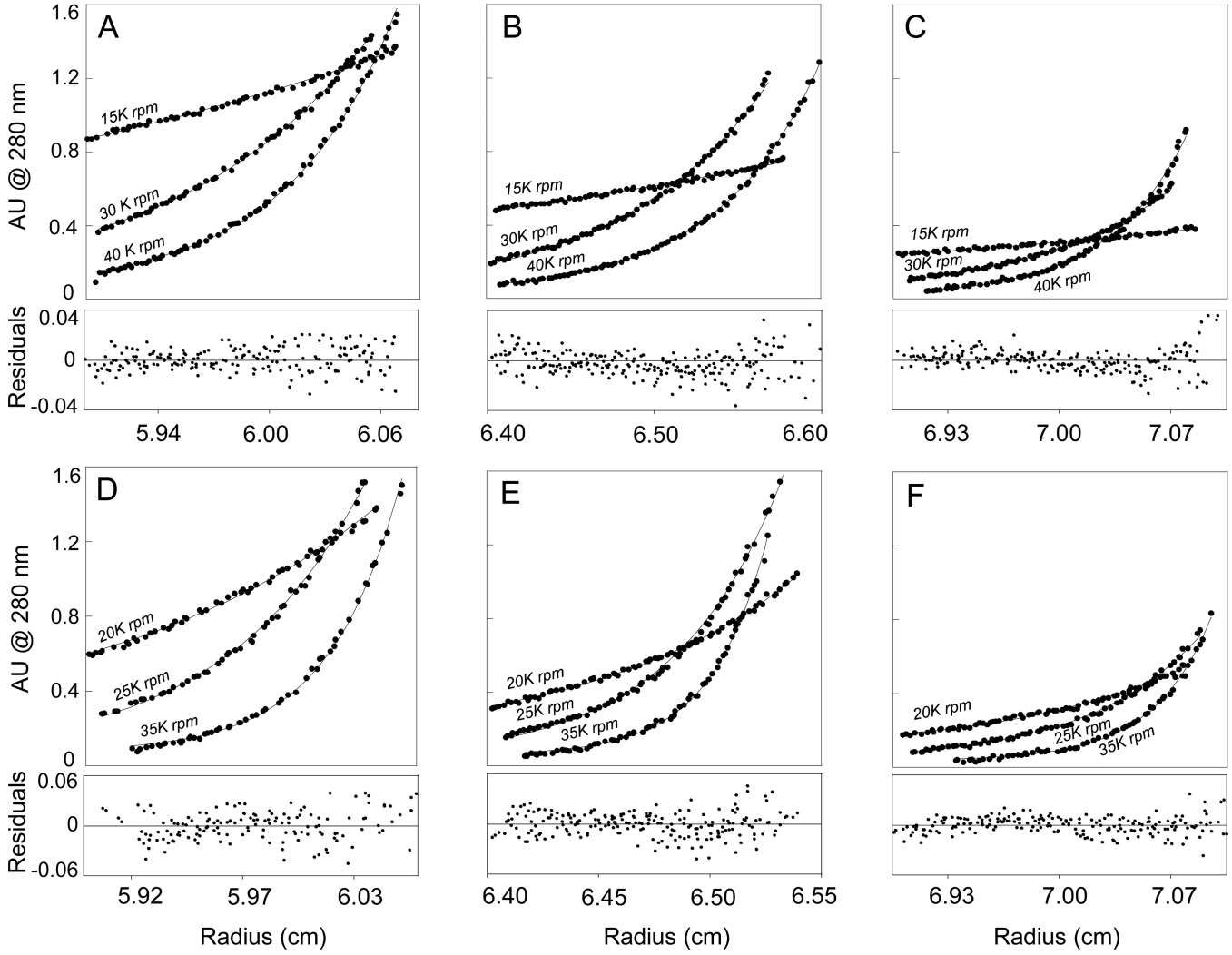

Figure 3.

Sedimentation equilibrium profiles of $Cav1_{62–178}$ and $Cav1_{62–178}$ P132L. Panels A–C represent the $Cav1_{62–178}$ at concentrations of 30 μM, 15 μM, and 7.5 μM, respectively. Panels D–F represent $Cav1_{62–178}$ P132L at concentrations of 30 μM, 15 μM, and 7.5 μM, respectively. Both wild type and mutant were evaluated at three speeds which have been overlayed in each panel.

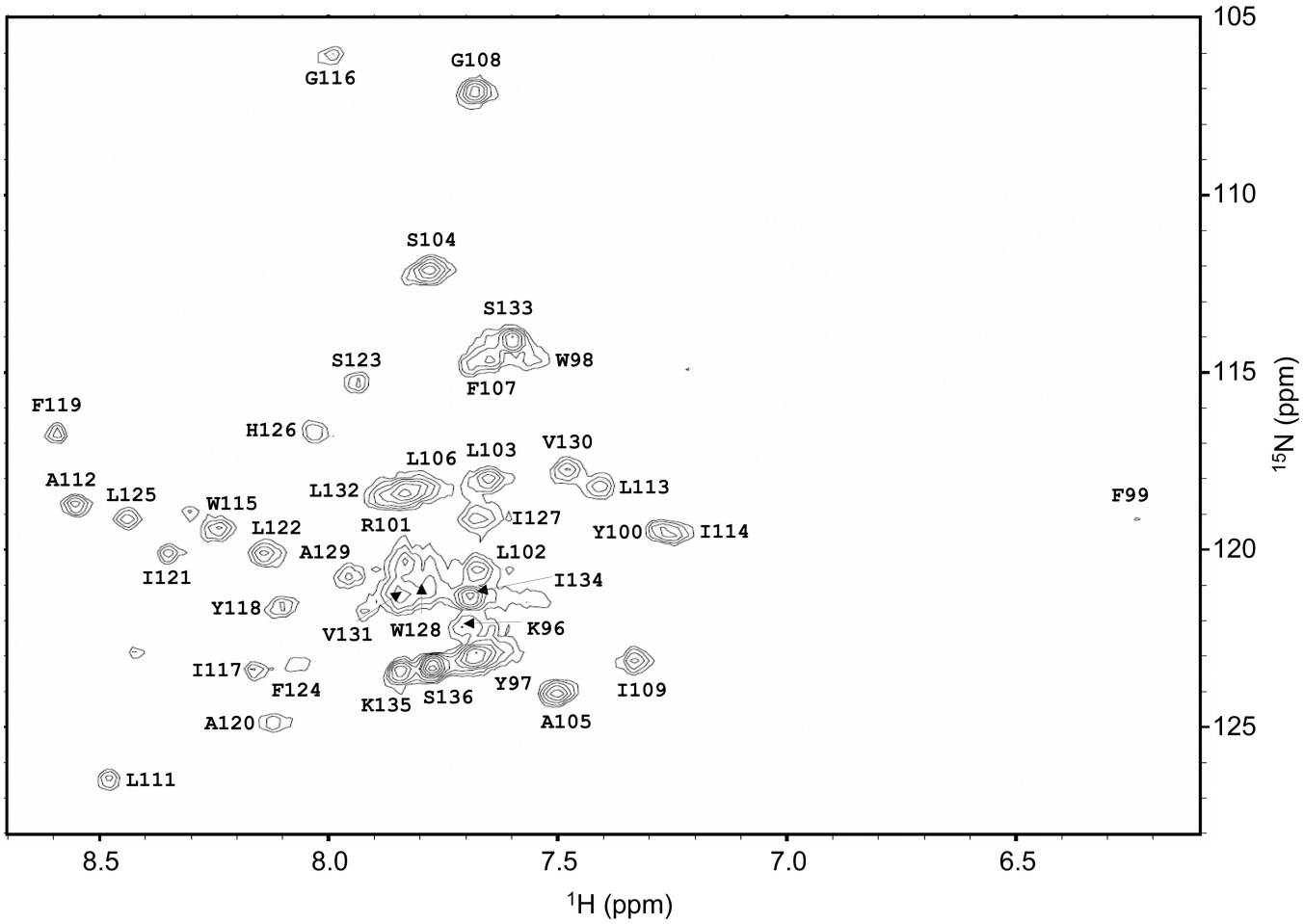

Figure 4.

^{1}H-^{15}N TROSY HSQC spectrum of Cav1$_{96–136}$ P132L. The spectrum was acquired with 256 complex points in t1 (^{15}N) and 2048 complex points in t2 (^{1}H).

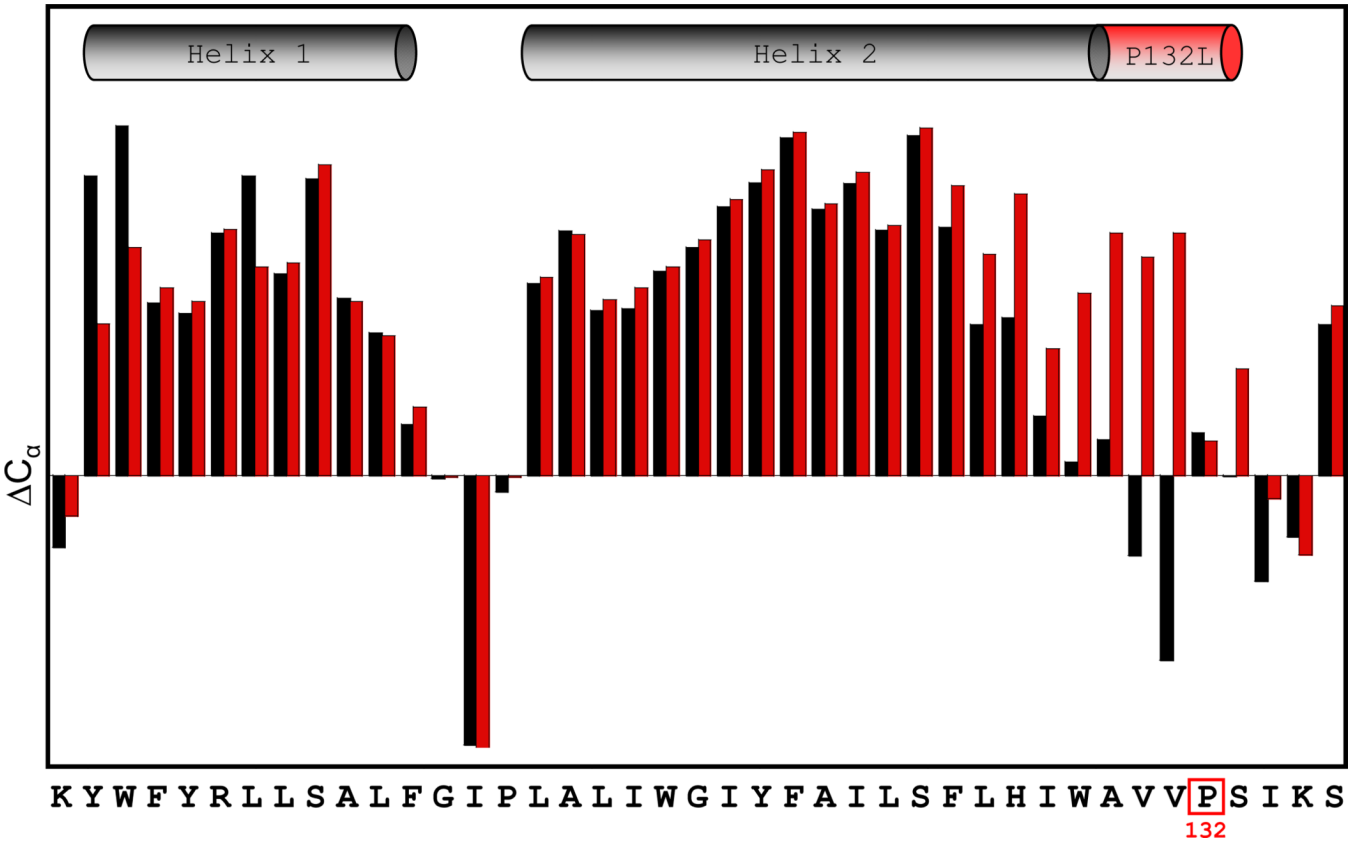

Figure 5.

Chemical shift analysis of $Cav1_{96–136}$ and $Cav1_{96–136}$ P132L. Wild type is depicted with black bars and the mutant is depicted with red bars. $Cav1_{96–136}$ P132L shows an extension of helix 2 by four residues.

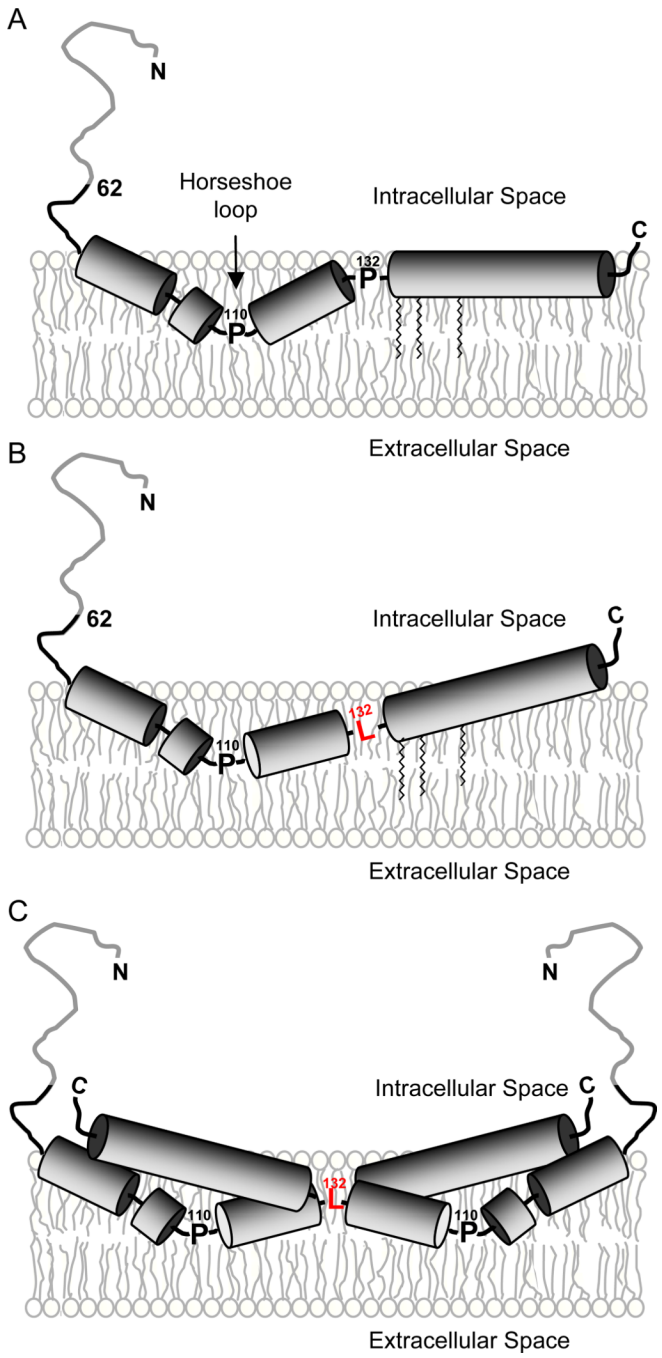

Figure 6.
Model of caveolin-1 in the plasma membrane. B) Model of caveolin-1 P132L mutant in the plasma membrane. C) Model of the caveolin-1 P132L dimer.

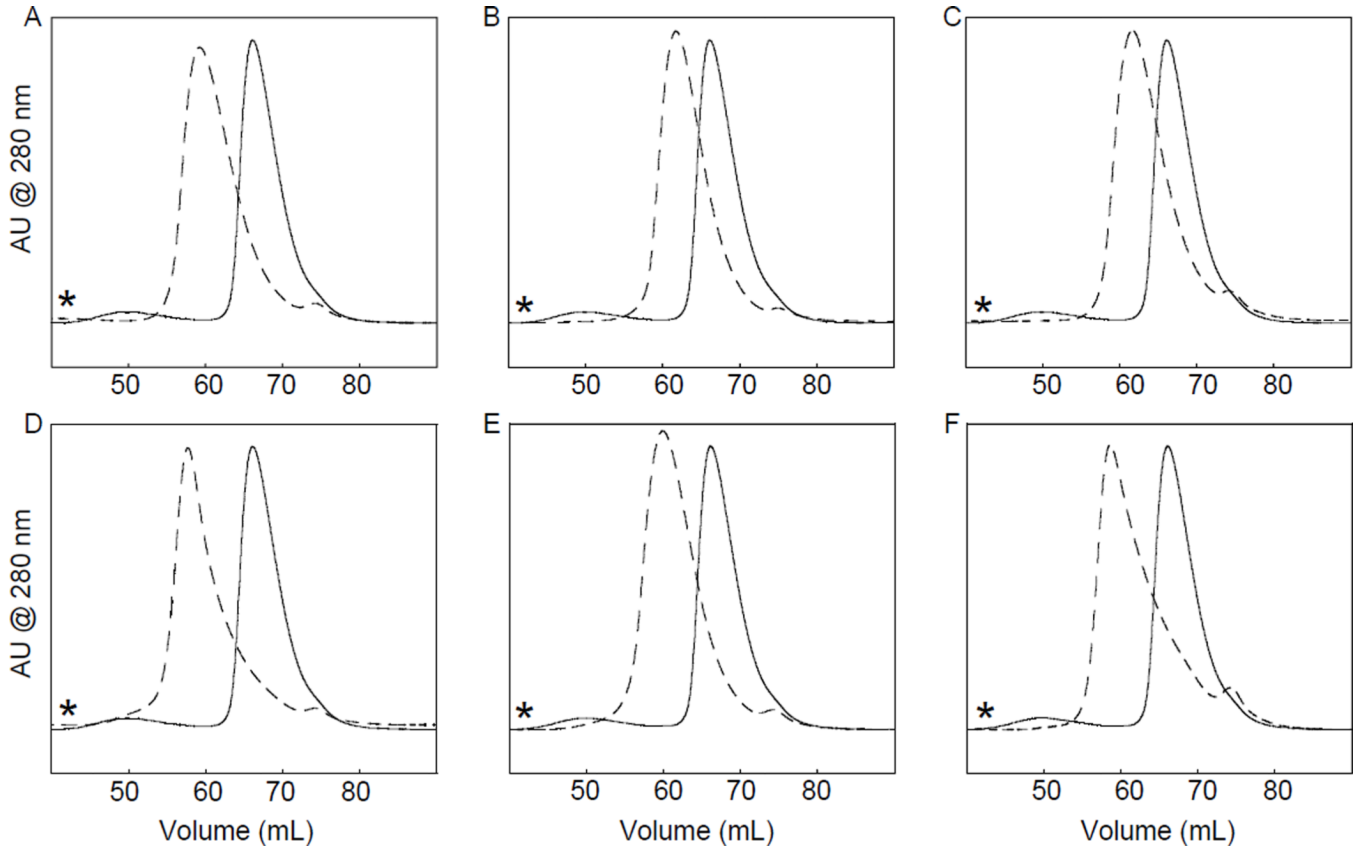

Figure 7.
Gel filtration chromatograms of the caveolin-1 P132X mutants. A) P132I B) P132G C) P132A D) P132F E) P132V F) P132W. The dashed line represents the P132X mutant and the solid line represents the wild type.